



⁶⁸Ga-PSMA-11 PET/CT combining ADC value of MRI in the diagnosis of naive prostate cancer

Perspective of radiologist

Liwei Wang, MD, PhD^a, Fei Yu, MD^b, Lulu Yang, MD^c, Shiming Zang, MD^b , Hailin Xue, MD^a, Xindao Yin, MD, PhD^a, Hongqian Guo, MD, PhD^d, Hongbin Sun, MD, PhD^{e,*} , Feng Wang, MD, PhD^{b,*}

Abstract

⁶⁸Ga-PSMA-11 positron emission computed tomography /computed tomography (PET/CT) is more sensitive than magnetic resonance imaging (MRI) in detecting prostate cancer (PCa). We evaluated the value of ⁶⁸Ga-PSMA-11 PET/CT with MRI in treatment-naive PCa.

This retrospective study was approved by the hospital ethics committee. The MRI and ⁶⁸Ga-PSMA-11 PET/CT imaging data of 63 cases of highly suspected PCa were enrolled in this study. The SUV_{max} and apparent diffusion coefficient (ADC), and their ratio, were assessed as diagnostic markers to distinguish PCa from benign disease.

There were 107 prostate lesions detected in 63 cases. Forty cases with 64 malignant primary lesions were confirmed PCa, whereas 23 cases had 43 benign lesions. PSMA-avid lesions correlated with hypointense signal on ADC maps and hyperintense signal on diffusion-weighted imaging. The ADC of PCa was lower than that of benign lesions, and SUV_{max} and SUV_{max}/ADC of PCa was higher than that of benign lesions ($P < .01$). ADC had significant negative correlation with Gleason score (GS) and SUV_{max}, SUV_{max}, and SUV_{max}/ADC positively correlated with GS. From ROC analysis, we established cutoff values of ADC, SUV_{max}, and SUV_{max}/ADC at $1.02 \times 10^{-3} \text{mm}^2/\text{s}$, 11.72, and 12.35, respectively, to differentiate PCa from benign lesions. The sensitivity, specificity, and AUC were 90.6%, 58.1%, and 0.816 for ADC, 67.2%, 97.7%, and 0.905 for SUV_{max}, and 81.2%, 88.4%, and 0.929 for SUV_{max}/ADC, respectively.

⁶⁸Ga-PSMA-11 PET/CT combined with MRI offers higher diagnostic efficacy in the detection of PCa than either modality alone.

Abbreviations: ADC = apparent diffusion coefficient, AUC = area under the curve, BPH = benign prostatic hyperplasia, DWI = diffusion-weighted imaging, GS = Gleason score, MRI = magnetic resonance imaging, PCa = prostate cancer, PET = positron emission computed tomography, PSMA = prostate-specific membrane antigen, TR = repetition time. T1WI = T1-weighted imaging, T2WI = T2-weighted imaging.

Keywords: magnetic resonance imaging (MRI), positron emission computed tomography (PET), prostate cancer, prostate-specific membrane antigen (PSMA)

1. Introduction

Magnetic resonance imaging (MRI) is recommended for the diagnosis of prostate cancer (PCa) in patients with a high pretest likelihood.^[1,2] Multiparametric MRI can reveal histopathological characteristics.^[3] MRI tends to detect high-risk

lesions or clinically significant PCa, which leads to prompt treatment. The apparent diffusion coefficient (ADC) generated by diffusion-weighted imaging (DWI) is a parameter for quantitative analysis of malignant lesions.^[4,5] Though ADC is helpful for tumor characterization, false-positive and false-negative findings are common.^[6] Therefore, ADC alone has

Editor: Giuseppe Lucarelli.

LW and FY contributed equally to this work.

This research was supported by grants from the National Natural Science Foundation of China (81271604), Jiangsu Provincial Nature Science Foundation (BL2012037, BK2011104), and Scientific and Medical Program in Nanjing (ZKX17027).

The authors have no conflicts of interest to disclose.

All data generated or analyzed during this study are included in this published article [and its supplementary information files].

^a Department of Radiology, ^b Department of Nuclear Medicine, ^c Department of Pathology, Nanjing First Hospital, Nanjing Medical University, ^d Department of Urology, Drum Tower Hospital, Medical School of Nanjing University, Nanjing University, ^e Department of Urology, Nanjing First Hospital, Nanjing Medical University, Nanjing, China.

* Correspondence: Feng Wang, Department of Nuclear Medicine, Nanjing First Hospital, Nanjing Medical University, 68th Changle Road, Nanjing 210006, China (e-mail: fengwangcn@hotmail.com); Hongbin Sun, Department of Urology, Nanjing First Hospital, Nanjing Medical University, 68th Changle Road, Nanjing 210006, China (e-mail: docshb@126.com).

Copyright © 2020 the Author(s). Published by Wolters Kluwer Health, Inc.

This is an open access article distributed under the terms of the Creative Commons Attribution-Non Commercial License 4.0 (CCBY-NC), where it is permissible to download, share, remix, transform, and buildup the work provided it is properly cited. The work cannot be used commercially without permission from the journal.

How to cite this article: Wang L, Yu F, Yang L, Zang S, Xue H, Yin X, Guo H, Sun H, Wang F. ⁶⁸Ga-PSMA-11 PET/CT combining ADC Value of MRI in the Diagnosis of Naive Prostate Cancer: Perspective of Radiologist. *Medicine* 2020;99:36(e20755).

Received: 3 March 2020 / Received in final form: 16 May 2020 / Accepted: 20 May 2020

<http://dx.doi.org/10.1097/MD.0000000000020755>

not become the single parameter with which to decide on biopsy.

Prostate-specific membrane antigen (PSMA) is an intrinsic transmembrane protein, which is highly expressed in 95% of PCa; its expression corresponds positively with the degree of malignancy.^[7,8] The improved efficacy of [⁶⁸Ga]-labeled PSMA with a ligand, such as PSMA-11 (also known as HBED-CC) and PSMA-617, has been well documented in the diagnosis of PCa.^[9,10] Our previous studies further demonstrated that it had higher sensitivity in the diagnosis of treatment-naïve PCa and primary staging, especially for lymphadenopathy.^[11–14] This technique allows prediction of biochemical recurrence and of lymphadenopathy, which has great impact on the clinical management.

The objective of this study was to evaluate the diagnostic value of ⁶⁸Ga-PSMA-11 positron emission computed tomography (PET/CT) and MRI in treatment-naïve PCa and investigate the feasibility of combining ADC from MRI and SUV_{max} from PET/CT in differentiation of PCa from benign disease.

2. Methods

2.1. Patients

Between December 2016 and September 2019, 428 patients with suspected PCa underwent ⁶⁸Ga-PSMA-11 PET/CT. A total of 95 patients underwent both ⁶⁸Ga-PSMA-11 PET/CT and MRI. Inclusion criteria for case data were: No treatment prior to examinations. PET/CT and MRI were performed within 2 weeks. Patients underwent radical prostatectomy or biopsy after imaging, with the final diagnosis confirmed by histopathology. Exclusion criteria: patients diagnosed with PCa previously; > 14 days between the 2 examinations; previous surgery or biopsy; disease not confirmed by pathology. A total of 63 cases met the

inclusion criteria. Mean age was 69.56 ± 11.56 years. A detailed flowchart is shown in Fig. 1. The prostate-specific antigen (PSA) levels ranged from 4.15 to 1298 ng/mL. This retrospective study was approved by the review board of our hospital. All patients signed written consents.

2.2. MRI acquisition protocol

MRI was performed with a high-field system (Intera Achieva 3.0T TX, Philips, The Netherlands). The sequences were as follows: transverse T1-weighted imaging (T1WI, repetition time [TR]=400 ms, echo time [TE]=10 ms, field-of-view [FOV]=35 × 30 cm, matrix=192 × 200); T2-weighted imaging (T2WI) (TR=3500 ms, TE=90 ms, FOV=20 × 20 cm, matrix=240 × 230); fat-suppression spectral presaturation attenuated inversion recovery-T2WI (TR=2800 ms, TE=100 ms, FOV=25 × 40 cm, matrix=270 × 200); DWI (TR=6200 ms, TE=2000 ms, FOV=20 × 30 cm, matrix=80 × 142, b=1500 s/mm²). The section thickness of each sequence was 3 mm; the section interval was 0.3 mm. Transverse DWI was obtained by single-shot echo planar imaging.

2.3. ⁶⁸Ga-PSMA-11 PET/CT

PSMA-11(HBED-CC) was purchased from ABX (Germany). ⁶⁸Ga-PSMA-11 was radiolabeled using the automated labeling module produced by ITM (Germany). The radiochemical purity was > 99%. The synthesis procedure was reported previously.^[11] Whole-body PET/CT (uMI780, United Imaging, China) was performed from the vertex to the proximal legs 1 hour postinjection of ⁶⁸Ga-PSMA-11 (111–185 MBq). Attenuation-corrected images were assessed clinically by certified nuclear medicine physicians.

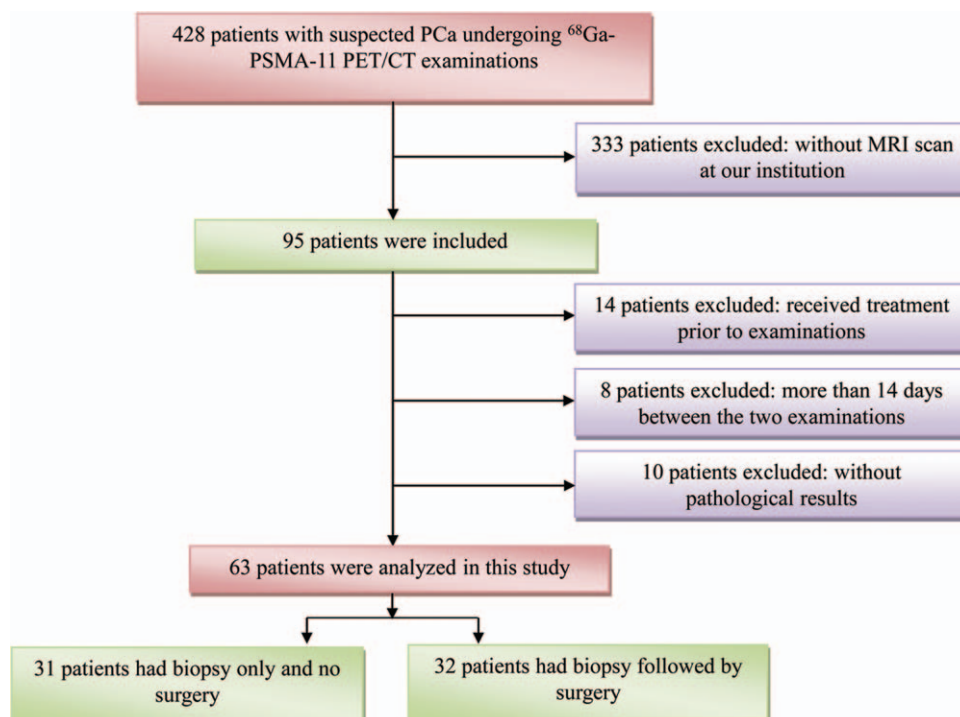


Figure 1. The flow chart of eligible case data inclusion.

2.4. Image interpretation

All MR images were interpreted by 1 certified radiologist (with 5 years of experience in prostate MRI) while blinded to PET images. Both interpreters reviewed all imaging data in a single session blinded to all clinical and pathologic data. Regions of interest were placed around lesions with diameters > 5 mm. The mean ADC and maximum SUV_{max} were measured. For ADC values, an ROI was drawn around the lesion on DWI according to hypointense signal on T2WI. The SUV_{max}/ADC ratio was manually calculated to express both PSMA expression and ADC.

2.5. Statistical analysis

Continuous variables with abnormal distribution are expressed as median (interquartile range). The correlation between SUV_{max} and ADC and correlation between GS and SUV_{max} , ADC, and SUV_{max}/ADC were evaluated by Spearman correlation analysis. The Wilcoxon rank-sum test was used to compare the difference in SUV_{max} , ADC, and SUV_{max}/ADC among different groups. Additionally, receiver operating characteristic curve (ROC) analysis was performed to evaluate the sensitivity, specificity, area under the curve (AUC), and cutoff value of each parameter. AUCs of the 3 parameters were compared by the z test. R (version 3.6.1) and MedCalc (version 15.0) statistical software programs were employed for all analysis. $P < .05$ was considered statistically significant.

3. Results

Out of 63 cases enrolled in this retrospective study (40 with PCa, 23 with benign prostatic disease), 32 cases were confirmed by postoperation pathology, and 31 cases were confirmed by needle biopsy. A total of 107 primary prostate lesions were found among the 63 cases. There were 2 to 4 lesions in 27 cases, and 36 solitary lesions. Eighteen cases with PCa had lymph node metastasis (28.57%) and 6 cases had bone metastasis (9.52%). All pelvic lymph node metastases were detected by PET/CT and MRI while all extraprostatic bone metastases were only detected by PET/CT.

PCa presented as hypointense signal in the peripheral zone or the central gland on T2WI, hypointense signal on ADC maps, and hyperintense signal on DWI. These findings corresponded to focal increased uptake in ^{68}Ga -PSMA-11-PET images (Fig. 2). Benign prostatic hyperplasia (BPH) presented as increased volumes in the transition zone and central zone with compression and thinning of the peripheral zone (Fig. 3). Mixed hypointense and hyperintense signals were observed on T2WI, and no obvious hypointense or hyperintense signals appeared on DWI and ADC maps. No significantly increased uptake was observed on ^{68}Ga -PSMA-11 PET/CT. Characteristics of prostatitis were hypointense signals in the central and peripheral zone on T2WI, isointense or hyperintense signal on DWI, and isointense or hypointense signal on ADC maps. ^{68}Ga -PSMA-11-PET/CT showed no or mildly diffuse uptake (Fig. 4).

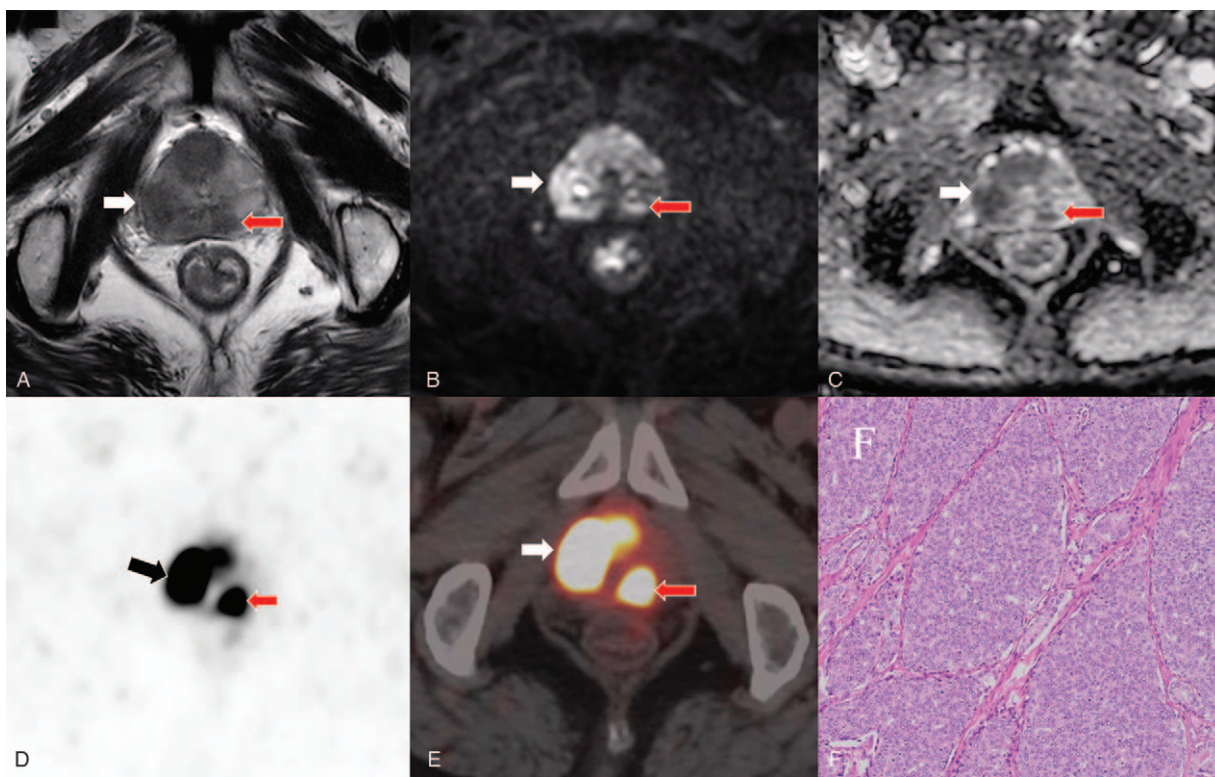


Figure 2. ^{68}Ga -PSMA-11 PET/CT and MRI in a case with progressive dysuria (male, age 83, PSA: 87.18 ng/mL). Hypointense signals were shown on T2WI (A, white and red arrows), and hyperintense signals on DWI (B, white and red arrows) in both lobes of prostate. ADC map showed hypointense signal in all lesions (C, white and red arrows). A PSMA-avid lesion occupies the right peripheral zone ($SUV_{max} = 33.19$, $SUV_{max}/ADC = 68.37$; D and E, white, black and red arrows). All of left and right lesions were confirmed pathologically as prostate cancer (HE staining, 100 \times magnification; GS 4 + 5 = 9; F). ADC = apparent diffusion coefficient, DWI = diffusion-weighted imaging, GS = Gleason score, MRI = magnetic resonance imaging, PET = positron emission computed tomography, PSMA = prostate-specific membrane antigen, SUV = standard uptake value, T2WI = T2-weighted imaging, PSA = prostate-specific antigen, CT = computed tomography.

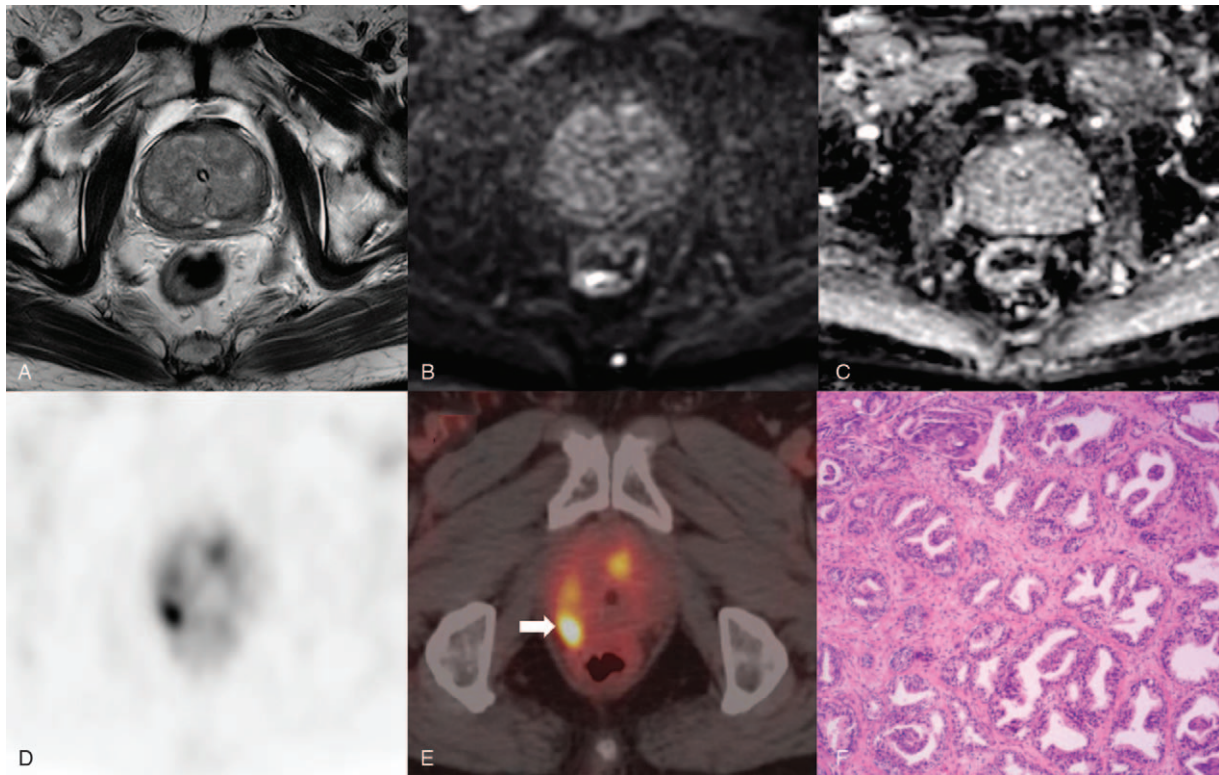


Figure 3. ^{68}Ga -PSMA-11 PET/CT and MRI in a case of benign prostatic hyperplasia (male, age 77, PSA: 66.07 ng/mL). T2WI showed prostatic hyperplasia in the central gland zone, with compression of the peripheral zone (A). No abnormal signals were identified on DWI or ADC map (B, C). ^{68}Ga -PSMA-11 PET/CT images showed concentrated radioactivity in the right peripheral zone ($\text{SUV}_{\text{max}}=13.86$, $\text{SUV}_{\text{max}}/\text{ADC}=10.67$; D and E, white arrow). Benign prostatic hyperplasia with prostatitis was confirmed by pathology (HE staining, 100 \times magnification; F). ADC = apparent diffusion coefficient, DWI = diffusion-weighted imaging, MRI = magnetic resonance imaging, PET = positron emission computed tomography, PSMA = prostate-specific membrane antigen, SUV = standard uptake value, T2WI = T2-weighted imaging, PSA = prostate-specific antigen, CT = computed tomography.

Five malignant prostatic lesions were missed on MRI but detected on ^{68}Ga -PSMA-11 PET/CT, which showed PSMA-avidity but no significant changes on DWI or ADC maps (Fig. 5).

The present study showed that ADC value negatively correlated with SUV_{max} ($P=1.52 \times 10^{-9}$ in all lesions, $P=4.54 \times 10^{-2}$ in benign lesions, and $P=7.94 \times 10^{-3}$ in PCa) (Fig. 6). The median (interquartile range) ADC values of benign and malignant lesions were 1.04 (0.75–1.29) and 0.69 (0.55–0.85), respectively. The median (interquartile range) SUV_{max} of benign lesions was 4.02 (3.00–7.86), and that of malignant lesions was 14.86 (9.34–19.80). The median (interquartile range) $\text{SUV}_{\text{max}}/\text{ADC}$ of benign lesions was 3.51 (2.67–6.15), whereas that of malignant lesions was 19.64 (13.12–33.16). The ADCs of PCa were significantly lower than those of benign disease ($P=3.27 \times 10^{-8}$), and SUV_{max} and $\text{SUV}_{\text{max}}/\text{ADC}$ of PCa were significantly higher than those of benign disease ($P=1.49 \times 10^{-12}$ and $P=6.33 \times 10^{-14}$, respectively), as shown in Table 1. For the 64 malignant lesions, the correlations between ADC, SUV_{max} , $\text{SUV}_{\text{max}}/\text{ADC}$ and Gleason score (GS) were analyzed. ADC negatively correlated with GS ($P=7.63 \times 10^{-4}$), while SUV_{max} and $\text{SUV}_{\text{max}}/\text{ADC}$ positively correlated with GS ($P=5.49 \times 10^{-9}$ and 1.71×10^{-10} , respectively) (Fig. 6). Stratified analysis found that ADC decreased in lesions with $\text{GS} > 6$ ($P=1.12 \times 10^{-2}$), and SUV_{max} and $\text{SUV}_{\text{max}}/\text{ADC}$ increased with $\text{GS} > 6$ ($P=7.14 \times 10^{-5}$) (Table 2).

From ROC analysis (Fig. 7), the cutoff value of ADC was determined to be $1.02 \times 10^{-3} \text{mm}^2/\text{s}$ for a sensitivity and specificity in PCa of 90.6% and 58.1%, respectively. The

Youden index was 0.49, and the AUC was 0.816. When the cutoff value for SUV_{max} was set at 11.72, the sensitivity and specificity of SUV_{max} in PCa was 67.2% and 97.7%, respectively, with a Youden index=0.65 and AUC=0.905. In ^{68}Ga -PSMA-PET/CT combined with MRI, a cutoff value for $\text{SUV}_{\text{max}}/\text{ADC}$ at 12.35 resulted in sensitivity and specificity of 81.2% and 88.4%, respectively. The Youden index=0.70, and the AUC=0.929. The AUCs of the 3 diagnostic parameters were compared by z test, and higher AUCs in SUV_{max} and $\text{SUV}_{\text{max}}/\text{ADC}$ than ADC alone were observed (Table 3).

4. Discussion

Transrectal ultrasound-guided percutaneous biopsy is a routine method in the diagnosis of PCa. However, the false-negative rate of biopsy is as high as 15% to 35%.^[15] MRI has improved the detection rate of clinically significant PCa, which avoids unnecessary biopsy. The ADC from DWI reflects the degree of diffusion of water molecules in the tissue. Current studies have shown that ADC maps illustrate the histopathological features of the lesion.^[16,17] ADC values were significantly lower in the PCa group than that in prostatitis, and ADC value alone showed high sensitivity in detecting PCa.^[18] However, the specificity of MRI for PCa is limited, and MRI likely missed some prostatic and extraprostatic lesions.

^{68}Ga -PSMA-11 PET has been validated to be more sensitive than MRI in the detection of PCa.^[19–24] SUV_{max} represents PSMA expression, which correlates with tumor differentiation

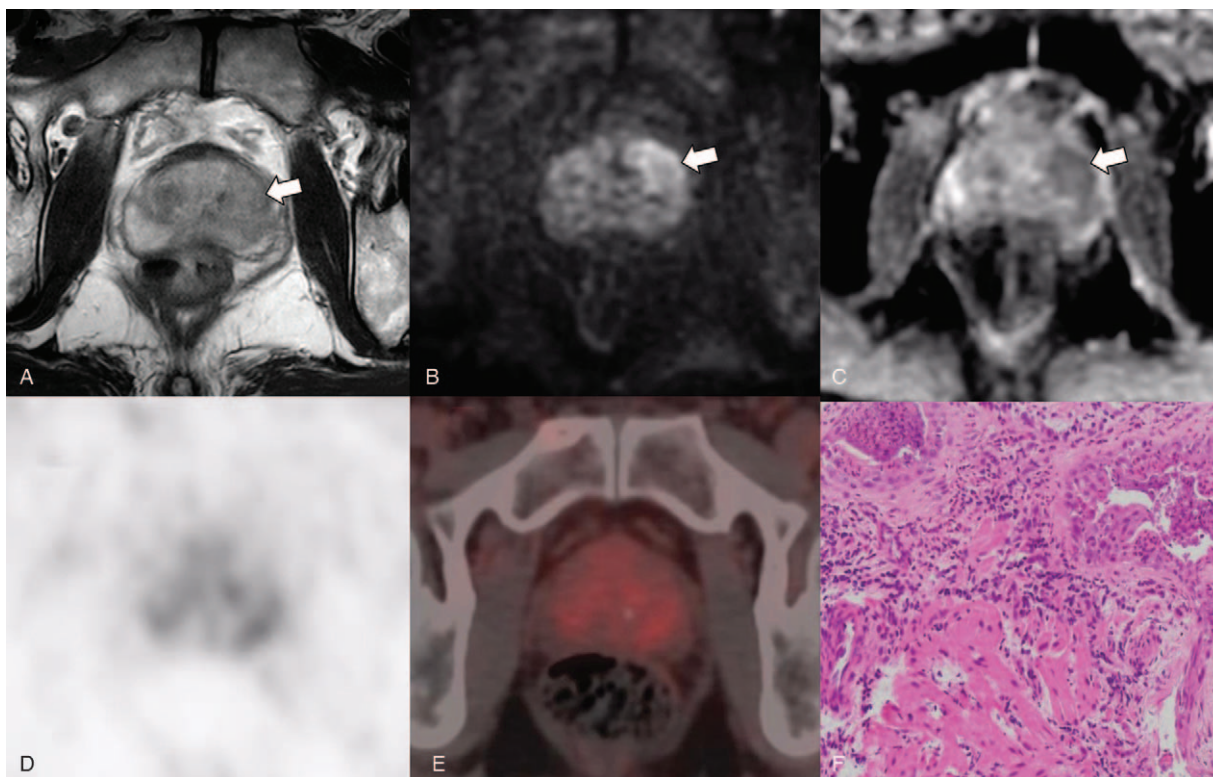


Figure 4. ^{68}Ga -PSMA-11 PET/CT and MR in a patient with prostatitis (male, age 65, PSA: 10.93 ng/mL). An irregular lesion with blurred borders in the left peripheral and transitional zones shown on T2WI (A, white arrow), slightly higher signal on DWI (B, white arrow), and low signal on ADC (C, white arrow). No obvious uptake in prostate gland ($\text{SUV}_{\text{max}}=4.66$, $\text{SUV}_{\text{max}}/\text{ADC}=5.18$; D and E). Benign prostatic hyperplasia with prostatitis was confirmed by pathology (HE staining, $100\times$ magnification; F). ADC = apparent diffusion coefficient, DWI = diffusion-weighted imaging, PET = positron emission computed tomography, PSMA = prostate-specific membrane antigen, SUV = standard uptake value, T2WI = T2-weighted imaging, PSA = prostate-specific antigen, CT = computed tomography.

and prognosis. The aim of this study was to investigate the diagnostic value of ^{68}Ga -PSMA-11 in treatment-naive prostate cancer compared with that of MRI, and the feasibility of using the $\text{SUV}_{\text{max}}/\text{ADC}$ was further explored. To our knowledge, this is the first head-to-head comparison study between MRI and ^{68}Ga -PSMA-11 PET in the detection of primary prostatic lesions in China.

In this study, the ADC value negatively correlated with SUV_{max} , which was consistent with previous studies.^[25,26] The $\text{SUV}_{\text{max}}/\text{ADC}$ ratio has been utilized to evaluate the combined advantages of MRI and PET/CT and showed great sensitivity and specificity for the detection of lymphadenopathy in PCa.^[25] This study demonstrated PCa was associated with lower ADC, and higher SUV_{max} and $\text{SUV}_{\text{max}}/\text{ADC}$. The GS negatively correlated with ADC values, and positively correlated with SUV_{max} and the $\text{SUV}_{\text{max}}/\text{ADC}$. These findings were consistent with other studies.^[27–30] $\text{SUV}_{\text{max}}/\text{ADC}$ may be used as a predictive parameter for PCa, to help distinguish benign from malignant prostatic lesions.

ROC curve analysis showed that ADC had high sensitivity but lower specificity in the detection of PCa. The sensitivity of SUV_{max} in this study (67.2%) was less than that reported in other studies,^[24,31,32] which may be attributed to differences among the populations and the different cutoff values. The ratio of $\text{SUV}_{\text{max}}/\text{ADC}$ integrates the degree of water molecule diffusion and PSMA expression. In this study, the diagnostic efficacy of the $\text{SUV}_{\text{max}}/\text{ADC}$ ratio was better than that of SUV_{max} or ADC alone. $\text{SUV}_{\text{max}}/\text{ADC}$ might be an alternative parameter in the detection of treatment-naive prostatic lesions.

MRI has been well documented in the detection of treatment naive prostate cancer, recent studies validated that MRI might improve the detection rate of clinical significantly PCa. However, MRI missed the lesion located in the transitional and ventral zone, especially patients combining with prostate hyperplasia. ^{68}Ga -PSMA-11 PET/CT had higher sensitivity in the detection of biochemical recurrence, several studies further validated that it improved the detection rate of primary prostatic lesion, especially in the peripheral and translational zone even with low PSA level. However, PSMA PET/CT missed some primary lesions in patients with higher Gleason Score or poor differentiated PCa and special rare PCa. Some false-positive or false-negative results existed in the clinical when SUV_{max} and ADC value are used separately. Therefore, as a radiologist, we supposed that SUV_{max} combining with ADC value might improve the detection rate of primary prostatic lesion. Combination of the SUV_{max} and ADC will decrease the deviation and improve the diagnostic accuracy.

In cases of high-GS primary PCa, ^{68}Ga -PSMA-11 PET/CT not only improved the detection rate of prostatic primary lesions but also of extra-prostatic spread, which had great impacts on staging and clinical management. To our great interest, 27 cases with multiple primary lesions were discovered in this study. MRI with ^{68}Ga -PSMA-11 PET/CT detected all lesions. From a radiology perspective, MRI is valuable in the detection of primary prostatic lesions in the peripheral and translational zone, and identification of seminal vesicle involvement. ^{68}Ga -PSMA-11 PET/CT has the advantage in the detection of multiple lesions and lesions in the central zone. ADC integration with ^{68}Ga -PSMA-11 PET/CT

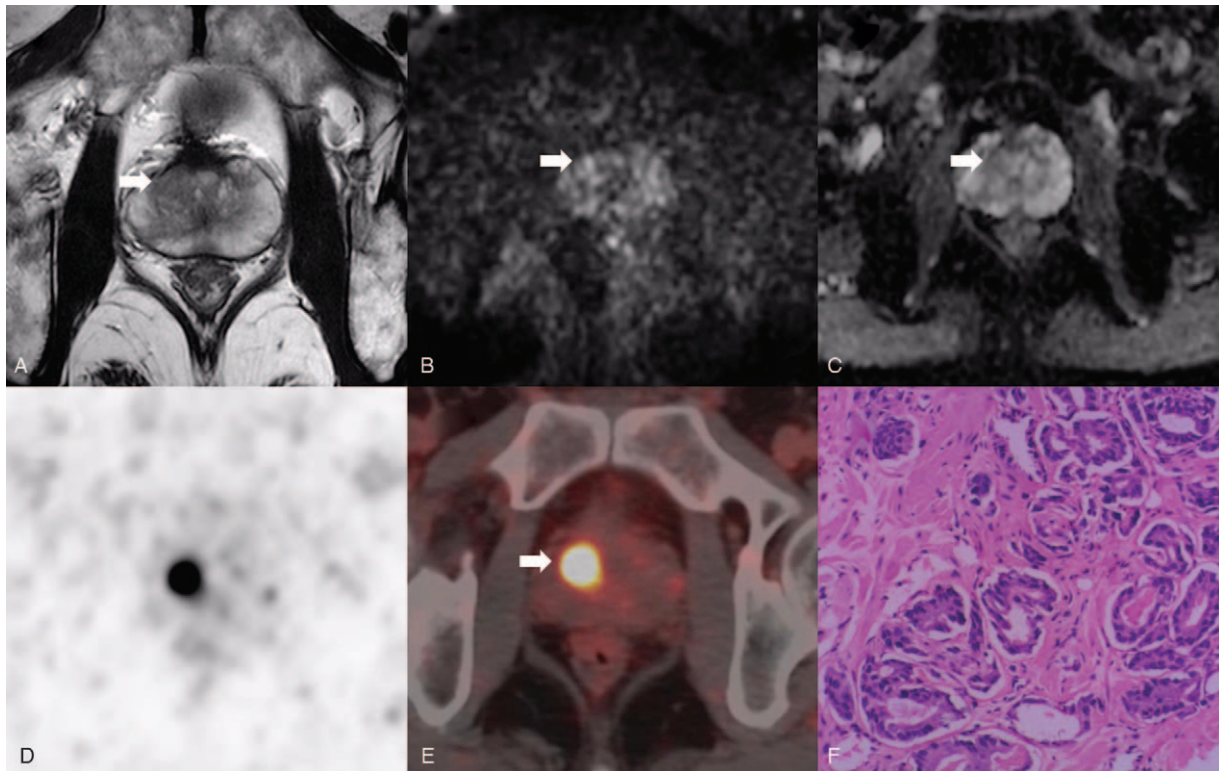


Figure 5. ^{68}Ga -PSMA-11 PET/CT detected a primary prostatic lesion, missed by MRI, in a case of suspected PCa (male, age 63, PSA: 17.57 ng/mL). Slightly hypointense signal in the right peripheral zone and transition zone are shown on T2WI (A, white arrow), isointense signal on DWI (B, white arrow), and slightly hypointense signal on ADC (C, white arrow). In ^{68}Ga -PSMA-11 PET/CT, obvious focal uptake in the right transition zone is shown ($\text{SUV}_{\text{max}} = 15.03$, $\text{SUV}_{\text{max}}/\text{ADC} = 17.68$; D and E, white arrow). Prostate cancer confirmed by pathology (HE staining, 100 \times magnification; GS 3 + 4 = 7; F). ADC = apparent diffusion coefficient, DWI = diffusion-weighted imaging, PET = positron emission computed tomography, PSMA = prostate-specific membrane antigen, SUV = standard uptake value, T2WI = T2-weighted imaging, PSA = prostate-specific antigen, CT = computed tomography, PCa = prostate cancer, GS = Gleason score.

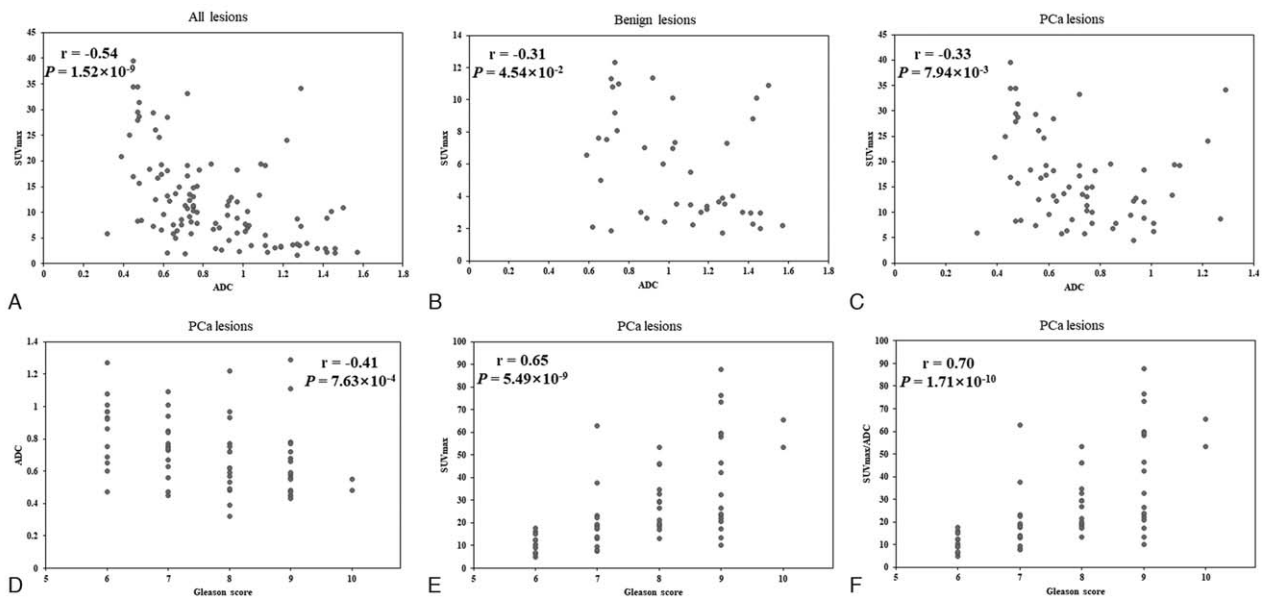


Figure 6. Scatter plots of the different parameters and GS. Correlation among SUV_{max} and ADC (A), benign lesions (B), and PCa lesions (C). Correlation among ADC and GS in PCa lesions (D), correlation between SUV_{max} and GS in PCa lesions (E), and correlation between $\text{SUV}_{\text{max}}/\text{ADC}$ and GS in PCa lesions (F). ADC = apparent diffusion coefficient, SUV = standard uptake value, PCa = prostate cancer, GS = Gleason score.

Table 1**The difference of the 3 diagnostic parameters.**

Parameter	Benign lesion	PCa lesion	W	P
ADC	1.04 (0.75, 1.29)	0.69 (0.55, 0.85)	2246	3.27×10^{-8}
SUV _{max}	4.02 (3.00, 7.86)	14.86 (9.34, 19.80)	262	1.49×10^{-12}
SUV _{max} /ADC	3.51 (2.67, 6.15)	19.64 (13.12, 33.16)	195	6.33×10^{-14}

ADC=apparent diffusion coefficient, SUVmax=standard uptake value.

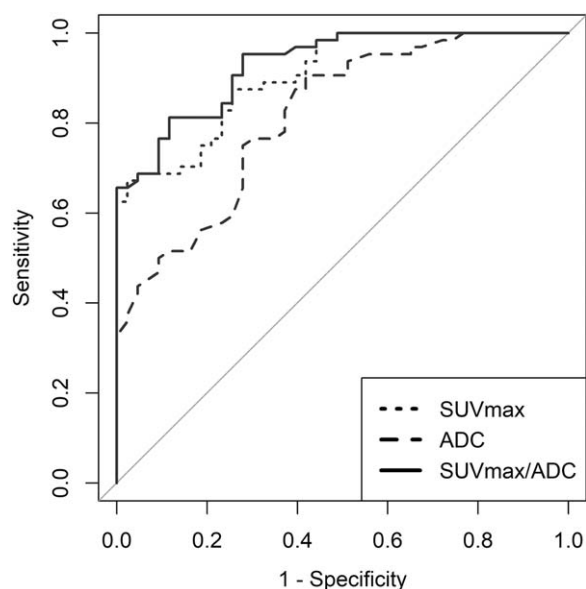
Table 2**The difference of the 3 diagnostic parameters between PCa with high (≥ 7) and low (≤ 6) GS.**

Parameter	GS(≤ 6)	GS(≥ 7)	W	P
ADC	0.92 (0.69, 0.97)	0.63 (0.51, 0.77)	484	1.12×10^{-2}
SUV _{max}	8.69 (7.90, 9.56)	17.37 (12.69, 24.79)	93	7.14×10^{-5}
SUV _{max} /ADC	10.32 (9.00, 12.47)	23.17 (17.60, 44.17)	62	7.16×10^{-6}

ADC=apparent diffusion coefficient, SUVmax=standard uptake value, GS=Gleason score.

provides some insights into the evaluation of tumor behavior and aggressiveness, with GS correlating positively with SUV_{max}/ADC. This study will pave the way for future investigations into the molecular phenotyping of prostate cancer.

The limitation of this study is that this was a small-scale retrospective study. Large-scale prospective studies between MRI and ⁶⁸Ga-PSMA-11 PET/CT in the detection of prostatic primary lesions are warranted in China. Second, this study was not performed with hybrid PET/MRI but with the modalities separated. A well-designed study with hybrid PET/MRI is underway. Third, we did not evaluate the role of SUV_{max}/ADC in predicting metastatic behavior on follow-up. In the future study, further study will be performed with simultaneous PET/MRI, which has been used in my department, SUV_{max}/ADC parameter will be further evaluated not only in prostatic primary

**Figure 7.** ROC curves of the 3 diagnostic parameters. ROC = receiver operating characteristic.**Table 3****Comparison of the AUCs of the 3 diagnostic parameters.**

Parameter	ADC and SUV _{max}	ADC and SUV _{max} /ADC	SUV _{max} and SUV _{max} /ADC
Z value	2.05	3.36	1.15
P	4.03×10^{-2}	8.00×10^{-4}	.13

ADC=apparent diffusion coefficient, AUC=area under the curve, SUVmax=standard uptake value.

lesion but also in metastatic lesion. We will validate if SUV_{max}/ADC can be served as a useful parameter for the evaluation of tumor biology and prognosis, which may have great impact of treatment strategy selection.

5. Conclusion

MRI combined with ⁶⁸Ga-PSMA-11 PET/CT has higher sensitivity and specificity for the diagnosis of treatment-naive PCa, which has great merits in the detection of multiple primary prostatic lesions and confirmation of seminal vesicle involvement. The SUV_{max}/ADC ratio may serve as a valuable parameter for the diagnosis of PCa and evaluation of biological behavior.

Acknowledgments

The authors thank all participants and staff from the Nanjing First Hospital for their contribution to the study.

Author contributions

Study design: Feng Wang, Liwei Wang.

Paper writing: Liwei Wang, Fei Yu.

Statistics and graphing: Fei Yu, Liwei Wang.

Histopathology: Lulu Yang.

PET/CT acquisition and interpretation: Shiming Zang, Feng Wang.

MRI acquisition and interpretation: Hailin Xue, Liwei Wang, Xindao Yin.

Patient biopsy and surgery: Hongbin Sun, Hongqian Guo.

References

- Woo S, Suh CH, Kim SY, et al. Head-to-head comparison between high- and standard-b-value DWI for detecting prostate cancer: a systematic review and meta-analysis. *AJR Am J Roentgenol* 2018;210:91–100.
- Barbieri S, Bronnimann M, Boxler S, et al. Differentiation of prostate cancer lesions with high and with low Gleason score by diffusion-weighted MRI. *Eur Radiol* 2017;27:1547–55.
- Taneja SS. Re: diagnostic accuracy of multi-parametric MRI and TRUS biopsy in prostate cancer (PROMIS): a paired validating confirmatory study. *J Urol* 2017;198:101–2.
- Kang Z, Min X, Weinreb J, et al. Abbreviated biparametric versus standard multiparametric MRI for diagnosis of prostate cancer: a systematic review and meta-analysis. *AJR Am J Roentgenol* 2019;212: 357–65.
- Papadopoulos I, Phillips J, Evans R, et al. Evaluation of diffusion weighted imaging in the context of multi-parametric MRI of the prostate in the assessment of suspected low volume prostatic carcinoma. *Magn Reson Imaging* 2018;47:131–6.
- Rourke E, Sunnapwar A, Mais D, et al. Inflammation appears as high prostate imaging-reporting and data system scores on prostate magnetic resonance imaging (MRI) leading to false positive MRI fusion biopsy. *Investig Clin Urol* 2019;60:388–95.
- Afshar-Oromieh A, Malcher A, Eder M, et al. PET imaging with a [⁶⁸Ga] gallium-labelled PSMA ligand for the diagnosis of prostate cancer: biodistribution in humans and first evaluation of tumour lesions. *Eur J Nucl Med Mol Imaging* 2013;40:486–95.

- [8] Koerber SA, Utzinger MT, Kratochwil C, et al. (68)Ga-PSMA-11 PET/CT in newly diagnosed carcinoma of the prostate: correlation of intraprostatic PSMA uptake with several clinical parameters. *J Nucl Med* 2017;58:1943–8.
- [9] Al-Bayati M, Grueneisen J, Lutje S, et al. Integrated 68Gallium labelled prostate-specific membrane antigen-11 positron emission tomography/magnetic resonance imaging enhances discriminatory power of multiparametric prostate magnetic resonance imaging. *Urol Int* 2018;100:164–71.
- [10] Freitag MT, Radtke JP, Afshar-Oromieh A, et al. Local recurrence of prostate cancer after radical prostatectomy is at risk to be missed in (68)Ga-PSMA-11-PET of PET/CT and PET/MRI: comparison with mpMRI integrated in simultaneous PET/MRI. *Eur J Nucl Med Mol Imaging* 2017;44:776–87.
- [11] Zang S, Shao G, Cui C, et al. 68Ga-PSMA-11 PET/CT for prostate cancer staging and risk stratification in Chinese patients. *Oncotarget* 2019;8:12247–58.
- [12] Chen M, Zhang Q, Zhang C, et al. Combination of (68)Ga-PSMA PET/CT and multiparametric MRI improves the detection of clinically significant prostate cancer: a lesion-by-lesion analysis. *J Nucl Med* 2019;60:944–9.
- [13] Gao J, Zhang Q, Zhang Q, et al. Diagnostic performance of (68)Ga-PSMA PET/CT for identification of aggressive cribriform morphology in prostate cancer with whole-mount sections. *Eur J Nucl Med Mol Imaging* 2019;46:1531–41.
- [14] Zhang Q, Zang S, Zhang C, et al. Comparison of ⁶⁸Ga-PSMA-11 PET-CT with mpMRI for preoperative lymph node staging in patients with intermediate to high-risk prostate cancer. *J Transl Med* 2017;15:230.
- [15] Eskicorapci SY, Guliyev F, Islamoglu E, et al. The effect of prior biopsy scheme on prostate cancer detection for repeat biopsy population: results of the 14-core prostate biopsy technique. *Int Urol Nephrol* 2007;39:189–95.
- [16] Kwak JT, Sankineni S, Xu S, et al. Prostate cancer: a correlative study of multiparametric MR imaging and digital histopathology. *Radiology* 2017;285:147–56.
- [17] Syer TJ, Godley KC, Cameron D, et al. The diagnostic accuracy of high b-value diffusion- and T2-weighted imaging for the detection of prostate cancer: a meta-analysis. *Abdom Radiol (NY)* 2018;43:1787–97.
- [18] Peker E, Sonmez DY, Akkaya HE, et al. Diagnostic performance of multiparametric MR imaging at 3.0 tesla in discriminating prostate cancer from prostatitis: a histopathologic correlation. *Eurasian J Med* 2019;51:31–7.
- [19] Calais J, Cao M, Nickols NG. The utility of PET/CT in the planning of external radiation therapy for prostate cancer. *J Nucl Med* 2018;59:557–67.
- [20] Taneja S, Jena A, Taneja R, et al. Effect of combined (68)Ga-PSMAHBED-CC uptake pattern and multiparametric MRI derived with simultaneous PET/MRI in the diagnosis of primary prostate cancer: initial experience. *AJR Am J Roentgenol* 2018;210:1338–45.
- [21] Herrmann K, Bluemel C, Weineisen M, et al. Biodistribution and radiation dosimetry for a probe targeting prostate-specific membrane antigen for imaging and therapy. *J Nucl Med* 2015;56:855–61.
- [22] Sachpekidis C, Kopka K, Eder M, et al. 68Ga-PSMA-11 dynamic PET/CT imaging in primary prostate cancer. *Clin Nucl Med* 2016;41:e473–9.
- [23] Giesel FL, Sterzing F, Schlemmer HP, et al. Intra-individual comparison of (68)Ga-PSMA-11-PET/CT and multi-parametric MR for imaging of primary prostate cancer. *Eur J Nucl Med Mol Imaging* 2016;43:1400–6.
- [24] Zhang J, Shao S, Wu P, et al. Diagnostic performance of (68)Ga-PSMA PET/CT in the detection of prostate cancer prior to initial biopsy: comparison with cancer-predicting nomograms. *Eur J Nucl Med Mol Imaging* 2019;46:908–20.
- [25] Uslu-Besli L, Bakir B, Asa S, et al. Correlation of SUV_{max} and apparent diffusion coefficient values detected by Ga-68 PSMA PET/MRI in primary prostate lesions and their significance in lymph node metastasis: preliminary results of an on-going study. *Mol Imaging Radionucl Ther* 2019;28:104–11.
- [26] Wetter A, Lippner C, Nensa F, et al. Quantitative evaluation of bone metastases from prostate cancer with simultaneous [18F] choline PET/MRI: combined SUV and ADC analysis. *Ann Nucl Med* 2014;28:405–10.
- [27] Ma XZ, Lv K, Sheng JL, et al. Application evaluation of DCE-MRI combined with quantitative analysis of DWI for the diagnosis of prostate cancer. *Oncol Lett* 2019;17:3077–84.
- [28] Park SY, Oh YT, Jung DC, et al. Diffusion-weighted imaging predicts upgrading of Gleason score in biopsy-proven low grade prostate cancers. *BJU Int* 2017;119:57–66.
- [29] Ergül N, Yılmaz Güneş B, Yücetaş U, et al. 68Ga-PSMA-11 PET/CT in newly diagnosed prostate adenocarcinoma. *Clin Nucl Med* 2018;43:e422–7.
- [30] Jena A, Taneja R, Taneja S, et al. Improving diagnosis of primary prostate cancer with combined (68)Ga-prostate-specific membrane antigen-HBED-CC simultaneous PET and multiparametric MRI and clinical parameters. *AJR Am J Roentgenol* 2018;211:1246–53.
- [31] Basha MAA, Hamed MAG, Hussein O, et al. ⁶⁸Ga-PSMA-11 PET/CT in newly diagnosed prostate cancer: diagnostic sensitivity and interobserver agreement. *Abdom Radiol (NY)* 2019;44:2545–56.
- [32] Bettermann AS, Zamboglou C, Kiefer S, et al. [⁶⁸Ga]PSMA-11 PET/CT and multiparametric MRI for gross tumor volume delineation in a slice by slice analysis with whole mount histopathology as a reference standard—implications for focal radiotherapy planning in primary prostate cancer. *Radiother Oncol* 2019;141:214–9.